

CHROMSYMP. 2785

Thermospray mass spectral studies of pesticides

Temperature and salt concentration effects on the ion abundances in thermospray mass spectra

D. Volmer*, A. Preiss and K. Levsen

Department of Analytical Chemistry, Fraunhofer Institute of Toxicology and Aerosol Research, Nikolai-Fuchs-Strasse 1, W-3000 Hannover 61 (Germany)

G. Wünsch

Institute of Inorganic Chemistry and Analytical Chemistry, University of Hannover, Callinstrasse 3, W-3000 Hannover 1 (Germany)

ABSTRACT

The dependence of the ion abundances in the thermospray (TSP) mass spectra of several pesticides, including anilides, carbamates, N-heterocyclic and organophosphorus compounds and phenylureas on the vaporizer and the gas-phase temperatures and under collision-activated dissociation conditions was investigated. The results clearly demonstrate that fragmentation in the TSP mass spectra of the investigated pesticides was mainly caused by gas- or liquid-phase "chemical dissociation" reactions of neutral analyte molecules or, in some instances, of the quasi-molecular ions in the ion source or the vaporizer probe, probably induced by solvent or buffer ions which can be described by well defined mechanisms. A linear relationship was observed for most of those pesticides which showed combinations of the two quasi-molecular ions $[M + H]^+$ and $[M + NH_4]^+$, when the logarithm of the ion abundance ratio for the $[M + H]^+$ ion relative to the $[M + NH_4]^+$ ion was plotted against the reciprocal of the absolute temperature of the gas phase. It is shown that this dependence can be used to generate TSP mass spectra with mainly one quasi-molecular ion. This may be of value for selected-ion monitoring experiments, because the total ion current (*i.e.*, the sum of the $[M + H]^+$ and $[M + NH_4]^+$ ions) is less dependent on the gas-phase temperature than the ion currents of the individual quasi-molecular ions. It was found that additional adduct ions beside these quasi-molecular ions could be observed in the spectra of several pesticides for which the formation was limited to low gas-phase temperatures. In addition, the results for the investigated quaternary ammonium compounds clearly show that the addition of a volatile buffer salt to the mobile phase induces chemical reactions in the gas phase which have a strong influence on the ion abundances. However, addition of buffer salt was necessary to obtain intense signals although the compounds are already completely dissociated in the aqueous solvent and fragmentation was enhanced as the buffer concentration was raised.

INTRODUCTION

The increasing use of pesticides in agriculture and thus the resulting concern about residues from these compounds in food and drinking water demands the development of highly sensitive and selective methods for their determina-

tion at trace levels. Unfortunately, universal methods are not available. As a result of their thermal instability and polarity, many of these compounds are not amenable to analysis by GC or GC-MS. In many instances they can, however, be analysed by liquid chromatographic (LC) methods. The former lack of a sensitive and selective LC detector has been overcome by combining LC with mass spectrometry (LC-MS). LC-MS offers major advantages over GC-

* Corresponding author.

MS for analysing thermally labile and polar compounds [1,2]. Different types of LC–MS interfaces have been applied to the analysis of these compounds in the last decade, such as a moving belt [3,4], direct liquid introduction (DLI) [5,6], fast atom bombardment (FAB) [7], thermospray (TSP) [8–10] and, more recently, particle beam [11]. Among these different interfaces, the TSP technique is the one most widely used. Some major classes of pesticides including carbamates [12,13], organophosphorus [14–16] and quaternary ammonium compounds [17], phenylureas [18,19], phenoxy acids [18,20], triazines [13,21] and some other classes have been analysed by LC–TSP–MS.

We have developed an LC–TSP–MS method for the extraction, separation and determination of approximately 130 pesticides, including anilides, carbamates, phenylureas, phenoxy acids, oximes, organophosphorus and quaternary ammonium compounds, triazines and other N-heterocyclic compounds and some other classes in aqueous environmental samples. Special attention was paid to pesticides produced in the former German Democratic Republic (GDR): the application of most of these compounds has been prohibited in Germany since the beginning of 1993, but they may still be found in aqueous samples. For many of these compounds no methods for their determination at trace levels are available. Examples for GDR-specific pesticides are presented in this paper. A more detailed description of the extraction, chromatographic separation and determination of all investigated compounds will be presented in a following paper.

Apart from demonstrating the applicability of TSP for the identification of a wide variety of pesticides, another aim of this work was to investigate the dependence of the ion abundances in the TSP mass spectra of several pesticides on the gas-phase and vaporizer temperatures. An increase in these temperatures may lead to enhanced fragmentation, whereas a decrease often results in additional cluster ions with several pesticides, which is useful for confirming a tentative identification based on the quasi-molecular ion alone as TSP ionization often results in spectra with insufficient structural information (*i.e.*,

one or two ions). Many attempts have been made to overcome this problem by using, *e.g.*, filaments, discharge ionization or MS–MS techniques [22] and by using additives to the mobile phase [23]. Moreover, the complementary information gained from positive- and negative-ion TSP mass spectra may be used to obtain additional structural information. The work described here will demonstrate the usefulness of varying the gas-phase and the vaporizer temperatures for inducing controlled chemical reactions during TSP vaporization and ionization. Fragmentation pathways for several pesticides will be discussed. The effect of temperature on the formation of additional cluster ions will also be demonstrated. In addition, methods for enhancing the sensitivity of the TSP detection are presented for several pesticides, including the variation of interface temperatures and the variation of the concentration of the volatile buffer salt.

EXPERIMENTAL

Materials

Organic-free water (Millipore, Bedford, MA, USA) and HPLC-grade methanol (Riedel-de Haën, Hannover, Germany) were passed through a 0.45- μm filter (Satorius, Göttingen, Germany) before use. Analytical-reagent grade ammonium acetate and ammonium formate were obtained from Aldrich (Steinheim, Germany) and Riedel-de Haën, respectively. Standards of the pesticides were purchased from Riedel-de Haën and Promochem (Wesel, Germany). They were of purity >98% and were used as received. Buminafos and butonate were a gift from Dr. J. Efer (University of Leipzig, Leipzig, Germany). Stock standard solutions of the chemicals were made up individually in methanol. From these stock standard solutions, serial dilutions with methanol or the mobile phase were made to obtain working standard solutions. PEG-300 and PEG-400 were purchased from Fluka (Buchs, Switzerland).

Liquid chromatography

The LC system consisted of a Varian (Palo Alto, CA, USA) Model 5000 gradient liquid chromatograph and a Shimadzu (Duisburg, Ger-

many) Model LC-9A pump for the postcolumn addition of buffer solution. The connection between the column and the TSP interface consisted of a low-dead-volume tee (Valco, Houston, TX, USA), a Rheodyne (Cotati, CA, USA) Model 7125 injector with a 50- μ l sample loop for flow injections and a 2- μ m screen filter (Valco). The buffer solution and the mass calibration mixture were added postcolumn through the tee. For chromatographic separations the samples were injected with a second Rheodyne injector equipped with a 20- μ l loop and separated with methanol–water gradient mixtures using a narrow-bore Nucleosil C₁₈ (5 μ m) column (125 \times 3 mm I.D.) (Machery–Nagel, Düren, Germany). A final flow-rate of 1.2 ml min⁻¹ in the TSP vaporizer was used in all experiments. A flow-rate of 0.6 ml min⁻¹ was maintained through the column, while 0.6 ml min⁻¹ of 150 mM aqueous buffer solution was added post-column. As the percentage of organic modifier in aqueous solvent mixtures strongly affects the sensitivity of the thermospray ionization, the post-column technique ensures that the final composition of the vaporized liquid varies only slightly (with a constant value of added salt), thus resulting in limits of detection that are virtually independent of the composition of the gradient mixture. The use of a high water content in the final solvent leads to a significant increase in TSP sensitivity. This increase can be attributed to the increase in the dielectric constant of the solvent as the water fraction is raised [24]. There is a second advantage of postcolumn buffer addition: the liquid chromatographic separation and TSP ionization analysis can be optimized separately, thus avoiding the possible negative influence of the precolumn addition of buffer on the chromatographic separation [25,26].

Mass spectrometry

The TSP interface (Vestec, Houston, TX, USA) was installed on a Finnigan MAT (San José, CA, USA) Model 4500 mass spectrometer. All experiments were performed with a 125- μ m tip-diameter vaporizer. Both the vaporizer and the source jet temperature were monitored. It is not clear which of the measured temperatures reflects the “gas-phase” temperature T_g and the

“reaction” temperature, *i.e.*, the temperature at which the gas-phase ion–molecule reactions occur. With the Vestec source, a thermocouple at the position of the repeller electrode would allow the closest measurement of this temperature. For calculations reported below, T_g can be approximated by the source jet (= vapour) temperature which is measured beyond the ion exit orifice because the difference between the source (“block”) temperature and the source jet temperature is small in most instances, typically between 10 and 20°C. In future experiments, a further thermocouple that will replace the repeller electrode will be used. The term T_g used below refers to the source jet temperature.

Typical operating conditions of the thermospray interface were as follows: vaporizer control temperature T_1 , *ca.* 135–150°C; vaporizer temperature T_v , *ca.* 190–210°C; vaporizer tip temperature T_3 , 270°C; source temperature T_s , 250°C; source jet temperature T_g , *ca.* 230–240°C; and exit line pressure p_g , *ca.* 2–4 Torr (1 Torr = 133.322 Pa) (the pressure is strongly dependent on the composition of the mobile phase and the flow-rate). For all variations of T_g , T_3 was set to the actual value of T_s , while T_v was kept constant. The mass spectrometer was operated in the positive-ion (PI) and negative-ion (NI) modes. The vaporizer temperature was optimized before each analysis to obtain a stable maximum ion intensity of the solvent cluster ions in the range m/z 18–139 for the positive ions and m/z 59–183 for the negative ions. The presence of these cluster ions limited the lower mass range available in TSP analysis. In this work, scanning was in general restricted to m/z values \geq 140 (PI) and \geq 185 (NI). The mass spectrometer was scanned at a rate of 1 s per scan over the mass range m/z 140–450 (PI) and 185–450 (NI).

The mass scale was calibrated with an aqueous solution of PEG-300 and PEG-400 containing 100 mM ammonium acetate, where the solution was continuously pumped into the TSP ion source. The polyethylene glycol–ammonium adduct ions were also used to tune the instrument.

LC–TSP–MS–MS experiments were performed on a Finnigan MAT TSQ 70 triple-stage quadrupole mass spectrometer (Q_1 , Q_2 , Q_3). In these MS–MS experiments, the $[M + H]^+$ or

$[M + NH_4]^+$ quasi-molecular ions were chosen as precursor ions and selectively transmitted by Q_1 for further collisional dissociation to Q_2 . Argon was used as the collision gas with a collision chamber pressure of $1.3 \cdot 10^{-3}$ Torr. A collision offset (COFF) of 10 V was applied to Q_2 . The collision-activated dissociation (CAD) daughter ions thus obtained were then analysed by scanning with the third quadrupole (Q_3) over the mass range m/z 10–300. For the LC–MS–MS studies, direct flow injection was used to introduce the samples into the mass spectrometer. The TSP vaporizer control temperature was set to 90°C and the aerosol temperature was kept at 240°C.

RESULTS AND DISCUSSION

Dependence of ion abundances in thermospray mass spectra on the vaporizer and gas-phase temperatures

TSP ionization of pesticides often results in mass spectra with insufficient structural information, *i.e.*, only the $[M + H]^+$ ion or the $[M + NH_4]^+$ ion or combinations of both ions appear in the spectra. However, in many instances it is possible to induce fragmentation by raising the vaporizer or the gas-phase temperature T_g . The examples in the following subsections will demonstrate that thermal decomposition is rare in TSP mass spectra of pesticides in the investigated temperature ranges of $T_g = 150$ – 320°C and $T_v = 140$ – 240°C . The degradation can be described by well defined reaction mechanisms. In addition, the dependence of the relative intensities of the quasi-molecular and cluster ion species on T_g was investigated. Relative abundances of the ions observed in the TSP mass spectra of the investigated compounds are summarized in Table I. Fig. 1 shows a full-scan TSP PI chromatogram of 26 pesticides under typical operating conditions.

Degradation reactions of organophosphorus pesticides. The TSP mass spectra of the investigated organophosphorus pesticides show a significantly increased fragmentation compared with other pesticides such as phenylureas and triazines. Special attention was paid to GDR-specific pesticides, *e.g.*, the phosphonic diesters

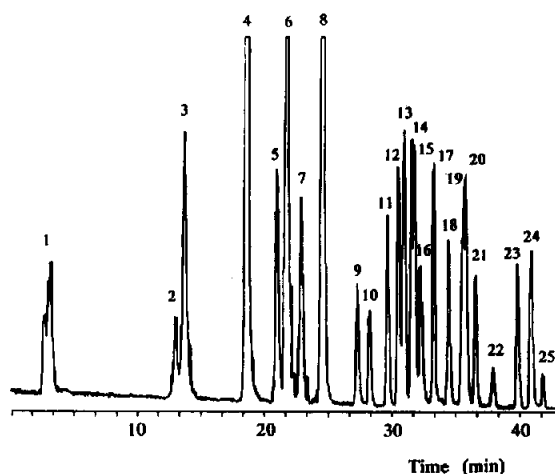


Fig. 1. Full-scan TSP PI chromatogram of several pesticides (180 ng each). Experimental conditions: filament-off, $T_v = 250^\circ\text{C}$, $T_g \approx 235^\circ\text{C}$ and $T_v = 205 \rightarrow 193^\circ\text{C}$ [gradient mixture: methanol–water, 10:90–90:10 (v/v), linear in 45 min; for details see Experimental]. Peak assignment: 1 = asulam; 2 = aldicarb sulphone; 3 = oxamyl; 4 = desisopropyl-atrazine; 5 = fenuron; 6 = dimethoate/metamitron; 7 = chloridazon; 8 = desethyl-atrazine; 9 = aldicarb; 10 = metoxuron; 11 = cyanazine; 12 = terbacil; 13 = monuron; 14 = carbofuran; 15 = simazine; 16 = hexazinon; 17 = carbaryl; 18 = monolinuron; 19 = chlorotoluron; 20 = atrazine; 21 = isoproturon; 22 = diuron; 23 = terbutylazine; 24 = propazine; 25 = chlorobromuron.

buminafos and butonate (the structures of which are shown in Figs. 2 and 5) and their degradation products. The investigated temperature range was $T_g = 150$ – 320°C .

Fig. 2 shows the TSP mass spectra of butonate at three different gas-phase temperatures (180, 235 and 300°C , $T_v = \text{constant}$). The quasi-molecular ion, $[M + NH_4]^+$, is the base peak in all instances, but a strong increase in the fragment ion abundance is observed as T_g is raised.

The fragmentation pathways suggested for butonate, the tentative structures of the fragments and the m/z values of the ions formed therefrom are shown in Fig. 3. The reaction starts with the hydrolysis of the phosphonic ester 1 to form trichlorfon (2), which after protonation or ammonium addition leads to the ions at m/z 257 and 274. In a second step, the elimination of HCl leads to the formation of dichlorvos (4) with the corresponding ions at m/z 221 and 238. This step probably involves an ylide-type electrophilic phosphor-to-oxygen 1,2-rearrangement of 3. Al-

TABLE I

DIRECT FLOW-INJECTION TSP POSITIVE-ION MASS SPECTRA OF THE INVESTIGATED PESTICIDES

Experimental parameters: $T_s = 250^\circ\text{C}$; $T_g = 235^\circ\text{C}$; $T_v = 202^\circ\text{C}$; mobile phase, MeOH–100 mM NH_4OAc (20:80); flow-rate, 1.2 ml min^{-1} ; the filament and the discharge electrode were not used in all experiments.

Compound	M_r	m/z (relative abundance, %)	Tentative identification
<i>Anilides</i>			
Alachlor	269	226 (62)	$[\text{M} + \text{H}_2\text{O} - \text{CH}_3\text{OCH}_2\text{OH} + \text{H}]^+$
		238 (36)	$[\text{M} - \text{CH}_2\text{OH} + \text{H}]^+$
		243 (70)	$[\text{M} + \text{H}_2\text{O} - \text{CH}_3\text{OCH}_3 + \text{NH}_4]^+$
		270 (100)	$[\text{M} + \text{H}]^+$
		287 (30)	$[\text{M} + \text{NH}_4]^+$
		305 ^a	$[\text{M} + \text{H}_2\text{O} + \text{NH}_4]^+$
		319 ^a	$[\text{M} + \text{MeOH} + \text{NH}_4]^+$
		329 ^a	$[\text{M} + \text{NH}_4\text{OAc} - \text{H}_2\text{O} + \text{H}]^+$
<i>Carbamates</i>			
Asulam	230	156 (4)	$[\text{M} - \text{CH}_3\text{OC}(\text{O})\text{NH}_2 + \text{H}]^+$
		173 (5)	$[\text{M} + \text{H}_2\text{O} - \text{CH}_3\text{OC}(\text{O})\text{OH} + \text{H}]^+$
		190 (100)	$[\text{M} + \text{H}_2\text{O} - \text{CH}_3\text{OC}(\text{O})\text{OH} + \text{NH}_4]^+$
		231 (5)	$[\text{M} + \text{H}]^+$
		248 (68)	$[\text{M} + \text{NH}_4]^+$
Carbaryl	201	145 (3)	$[\text{M} - \text{CH}_3\text{NCO} + \text{H}]^+$
		202 (18)	$[\text{M} + \text{H}]^+$
		219 (100)	$[\text{M} + \text{NH}_4]^+$
Carbofuran	221	165 (5)	$[\text{M} - \text{CH}_3\text{NCO} + \text{H}]^+$
		182 (3)	$[\text{M} - \text{CH}_3\text{NCO} + \text{NH}_4]^+$
		222 (100)	$[\text{M} + \text{H}]^+$
		239 (35)	$[\text{M} + \text{NH}_4]^+$
Chlorpropham	213	214 (20)	$[\text{M} + \text{H}]^+$
		231 (100)	$[\text{M} + \text{NH}_4]^+$
		249 ^a	$[\text{M} + 46]^+$
		263 ^a	$[\text{M} + \text{NH}_4\text{OAc} - 2\text{H}_2\text{O} + \text{NH}_4]^+$
Desmedipham	300	120 ^b	$[\text{M} - \text{C}_2\text{H}_5\text{OCONHC}_6\text{H}_4\text{OH} + \text{H}]^+$
		137 (20)	$[\text{M} - \text{C}_2\text{H}_5\text{OCONHC}_6\text{H}_4\text{OH} + \text{NH}_4]^+$
		182 (50)	$[\text{M} - \text{C}_6\text{H}_5\text{NCO} + \text{H}]^+$
		199 (100)	$[\text{M} - \text{C}_6\text{H}_5\text{NCO} + \text{NH}_4]^+$
		213 (7)	$[\text{M} - \text{C}_2\text{H}_5\text{OC}(\text{O})\text{NH} + \text{H}]^+$
		301 (<1)	$[\text{M} + \text{H}]^+$
Oxamyl	219	163 (33)	$[\text{M} - \text{CH}_3\text{NCO} + \text{H}]^+$
		180 (13)	$[\text{M} - \text{CH}_3\text{NCO} + \text{NH}_4]^+$
		220 (3)	$[\text{M} + \text{H}]^+$
		237 (100)	$[\text{M} + \text{NH}_4]^+$
Phenmedipham	300	134 ^b	$[\text{M} - \text{CH}_3\text{OC}(\text{O})\text{NHC}_6\text{H}_4\text{OH} + \text{H}]^+$
		151 (40)	$[\text{M} - \text{CH}_3\text{OC}(\text{O})\text{NHC}_6\text{H}_4\text{OH} + \text{NH}_4]^+$
		168 (45)	$[\text{M} - \text{C}_6\text{H}_5(\text{CH}_3)\text{NCO} + \text{H}]^+$

(Continued on p. 240)

TABLE I (continued)

Compound	M_r	m/z (relative abundance, %)	Tentative identification
		185 (100)	$[M - C_6H_5(CH_3)NCO + NH_4]^+$
		210 (17)	$[M - C_6H_5CH_3 + H]^+$
		301 (<1)	$[M + H]^+$
		318 (3)	$[M + NH_4]^+$
<i>Triazines and other N-heterocyclic compounds</i>			
Atrazine	215	216 (100)	$[M + H]^+$
		248 ^a	$[M + MeOH + H]^+$
		275 ^a	$[M + NH_4OAc - H_2O + H]^+$
Cyanazine	240	241 (100)	$[M + H]^+$
		273 ^a	$[M + MeOH + H]^+$
		300 ^a	$[M + NH_4OAc - H_2O + H]^+$
Terbacil	216	161 (23) ^c	$[M - CH_2=C(CH_3)_2 + H]^+$
		178 (100) ^c	$[M - CH_2=C(CH_3)_2 + NH_4]^+$
		217 (<1)	$[M + H]^+$
		234 (<1)	$[M + NH_4]^+$
<i>Organophosphorus compounds</i>			
Azinphos-ethyl	345	160 (100)	$[M - (C_2H_5)_2PS_2 + H]^+$
		346 (65)	$[M + H]^+$
		363 (33)	$[M + NH_4]^+$
Buminafos	347	154 (10)	$[M - HOP(OC_4H_9)_2 + H]^+$
		195 (30)	$[M - C_6H_5NHC_4H_9 + H]^+$
		212 (100)	$[M - C_6H_5NHC_4H_9 + NH_4]^+$
		293 (1)	$[M + H_2O - C_4H_9NH_2 + H]^+$
		348 (2)	$[M + H]^+$
Butonate	326	221 (1)	$[M + H_2O - C_3H_7CO_2H - HCl + H]^+$
		238 (2)	$[M + H_2O - C_3H_7CO_2H - HCl + NH_4]^+$
		257 (2)	$[M + H_2O - C_3H_7CO_2H + H]^+$
		274 (5)	$[M + H_2O - C_3H_7CO_2H + NH_4]^+$
		291 (15)	$[M - HCl + H]^+$
		308 (70)	$[M - HCl + NH_4]^+$
		327 (30)	$[M + H]^+$
		344 (100)	$[M + NH_4]^+$
Dichlorvos	220	221 (12)	$[M + H]^+$
		238 (100)	$[M + NH_4]^+$
		281 (5)	$[M + NH_4OAc - H_2O + H]^+$
Dimethoate	229	230 (100)	$[M + H]^+$
		247 (38)	$[M + NH_4]^+$
Disulfoton	274	275 (100)	$[M + H]^+$
		292 (10)	$[M + NH_4]^+$
Naled	380	221 (<1)	$[M - Br_2 + H]^+$
		238 (2)	$[M - Br_2 + NH_4]^+$
		381 (7)	$[M + H]^+$
		398 (100)	$[M + NH_4]^+$

TABLE I (continued)

Compound	M_r	m/z (relative abundance, %)	Tentative identification
Phorate	260	261 (100)	$[M + H]^+$
		278 (1)	$[M + NH_4]^+$
Phosmete	317	318 (35)	$[M + H]^+$
		335 (100)	$[M + NH_4]^+$
Trichlorfon	256	221 (1)	$[M - HCl + H]^+$
		238 (12)	$[M - HCl + NH_4]^+$
		257 (18)	$[M + H]^+$
		274 (100)	$[M + NH_4]^+$
<i>Phenylureas</i>			
Chlorotoluron	212	213 (100)	$[M + H]^+$
		230 (5)	$[M + NH_4]^+$
		245 ^a	$[M + MeOH + H]^+$
		258 ^a	$[M + 46]^+$
		271 ^a	$[M + NH_4OAc - 2H_2O + NH_4]^+$
		272 ^a	$[M + NH_4OAc - H_2O + H]^+$
Fenuron	164	165 (100)	$[M + H]^+$
		182 (40)	$[M + NH_4]^+$
		197 ^a	$[M + MeOH + H]^+$
		210 ^a	$[M + 46]^+$
Isoproturon	206	207 (100)	$[M + H]^+$
		224 (23)	$[M + NH_4]^+$
		239 ^a	$[M + MeOH + H]^+$
		252 ^a	$[M + 46]^+$
		265 ^a	$[M + NH_4OAc - 2H_2O + NH_4]^+$
<i>Quaternary ammonium compounds^d</i>			
Diquat	184 ^e	92 ^f (5)	$[Cat]^{2+}$
		157 (29)	$[Cat - CH_2CH_2 + H]^+$
		183 (6)	$[Cat - H]^+$
		184 (100)	$[Cat]^+$
		185 (23)	$[Cat + H]^+$
Paraquat	186 ^e	93 ^f (7)	$[Cat]^{2+}$
		157 (20)	$[Cat - 2CH_3 + H]^+$
		171 (5)	$[Cat - CH_3]^+$
		172 (100)	$[Cat - CH_3 + H]^+$
		186 (27)	$[Cat]^+$
		187 (84)	$[Cat + H]^+$
221 (1)	$[Cat + Cl]^+$		

^a These adduct ions were observed only at low gas-phase temperatures (see text).

^b CAD daughter ion spectrum.

^c The hydrolysis reaction in the vaporizer should also be considered (see text).

^d Cat = cation.

^e Nominal mass of the divalent cation (Cat^{2+}).

^f The intact dication is only observed in the TSP spectra with pure water as the solvent.

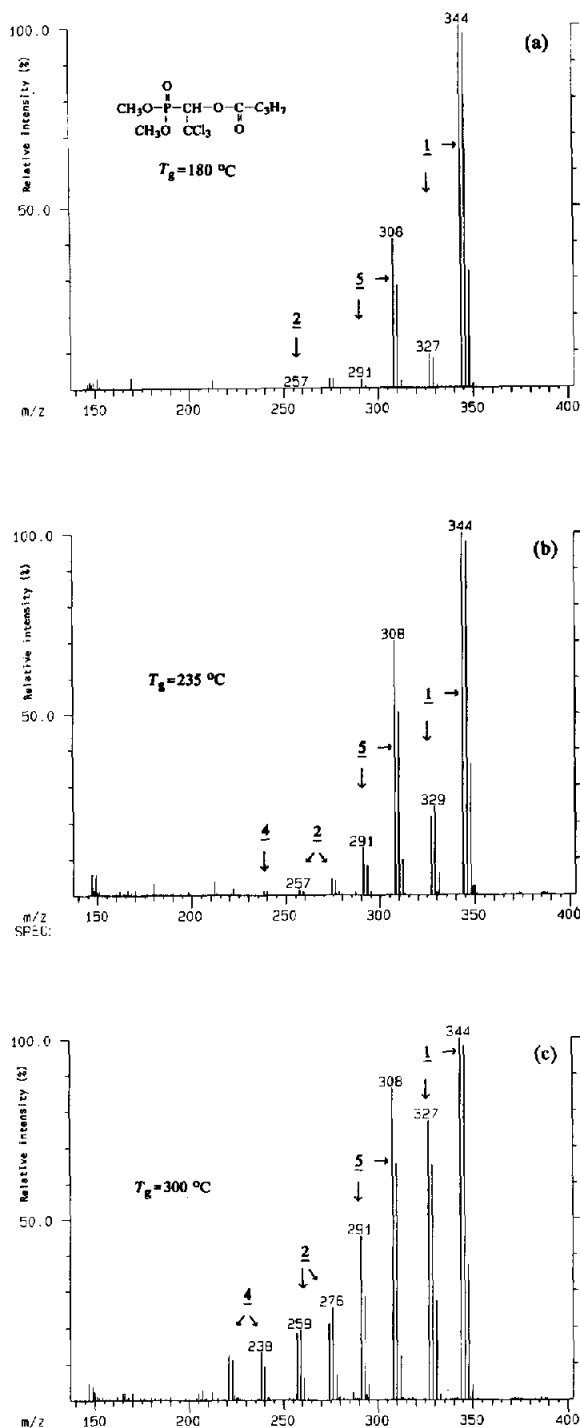


Fig. 2. Direct flow-injection TSP PI mass spectra of butonate for different gas-phase temperatures: T_g = (a) 180; (b) 235; (c) 300°C. Amount injected, 600 ng. The assignments of the tentative structures are shown in Fig. 3.

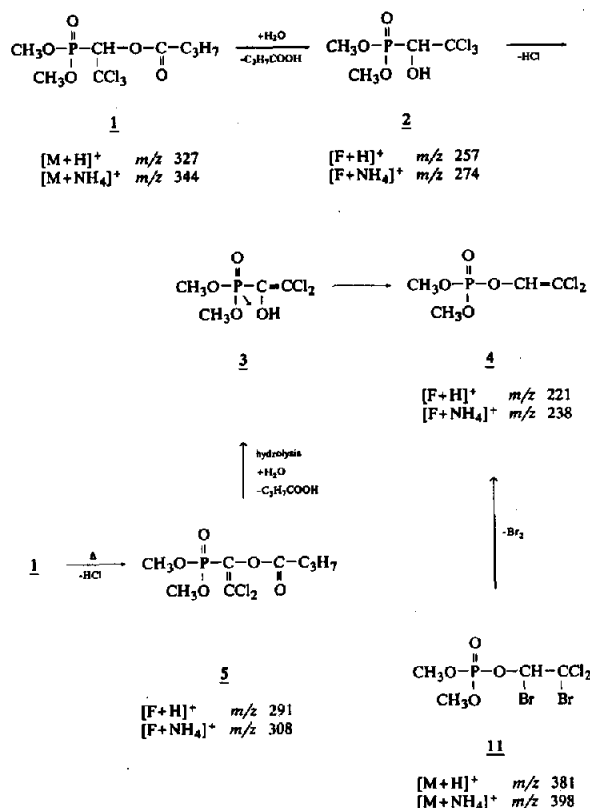


Fig. 3. Proposed fragmentation pathways for butonate and naled and observed ions in the TSP PI mass spectra.

ternatively, the fragmentation of 1 can also start with the direct elimination of HCl, which leads to the ions $[F+H]^+$ (m/z 291) and $[F+NH_4]^+$ (m/z 308), where F is a neutral fragment molecule. The corresponding ions from both reaction pathways are observed in the spectra in Fig. 1 (the HCl elimination in steps 2→3 and 1→5 was confirmed by the observed isotropic abundances of the chlorine atoms). The amount of fragmentation depends strongly on the gas-phase temperature, T_g (see Fig. 2a–c), while variation of the vaporizer temperature has only a slight influence. The conclusion that degradation of neutral butonate leads to the formation of trichlorophon and dichlorvos is corroborated on the one hand by a comparison with the TSP PI mass spectra of these two compounds which are shown in Fig. 4a and b for $T_g = 235^\circ\text{C}$. One observes that trichlorofon is degraded in the same manner as butonate to give dichlorvos. On the other

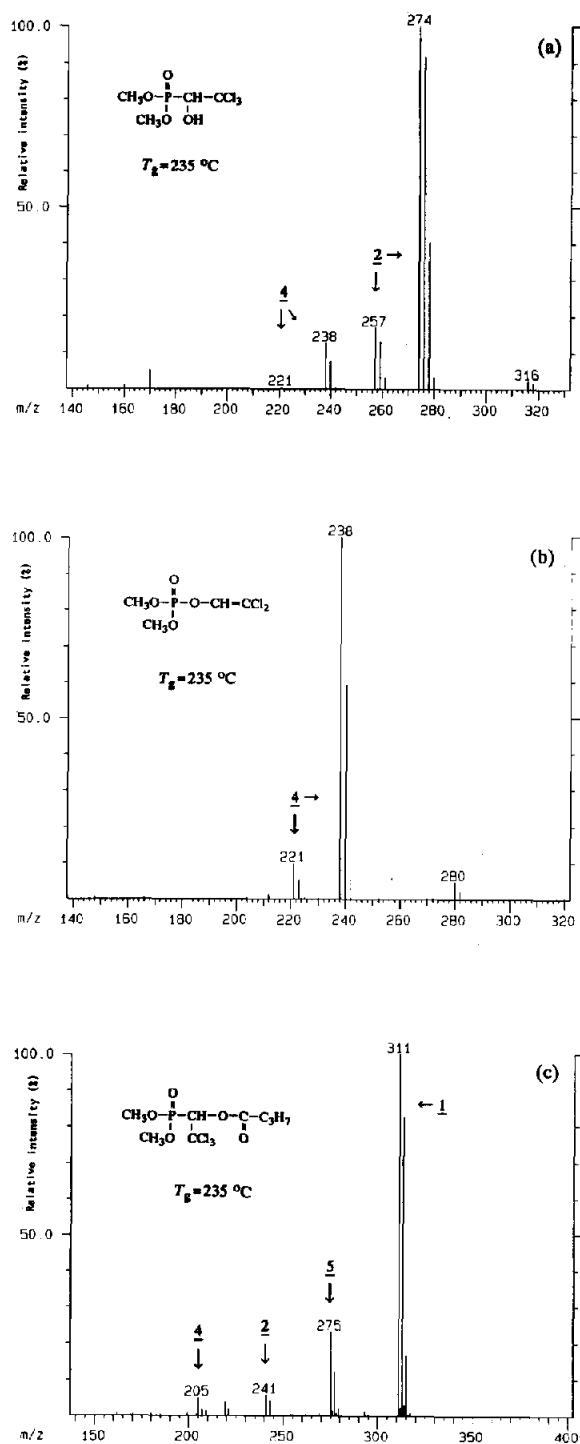


Fig. 4. TSP mass spectra of (a) trichlorfon (PI), (b) dichlorvos (PI) (amount injected, 600 ng) and (c) butonate (NI, filament-on, 2 μg) for $T_g = 235^\circ\text{C}$.

hand, further evidence for gas-phase and/or liquid-phase degradation processes is gleaned from the TSP NI spectra of butonate (Fig. 4c). In this mode, intense ions corresponding to $[\text{M} - \text{R}]^-$ or $[\text{F} - \text{R}]^-$ ions ($\text{R} = \text{CH}_3$) of 1, 2, 4 and 5 are observed which complement the $[\text{M} + \text{H}]^+$ and $[\text{M} + \text{NH}_4]^+$ or $[\text{F} + \text{H}]^+$ and $[\text{F} + \text{NH}_4]^+$ ions observed in the TSP PI mode. These ions are due to dissociative electron-capture reactions of neutral precursors [27]. This further demonstrates that when degradation products are formed from the neutral molecule, they readily produce quasi-molecular ions in both the PI and NI modes. If degradation products 2, 4 and 5 were produced by means of fragmentation of the quasi-molecular ions, it is unlikely that complementary fragment ions would appear in both the PI and NI spectra.

Dichlorvos is also formed by debromination of the pesticide naled, a phosphorus diester (11, see Fig. 3 and Table I). Again, both $[\text{M} + \text{H}]^+$ and $[\text{M} + \text{NH}_4]^+$ ions are formed, where the latter leads to the base peak. The fragment ion abundances are lower than for the other organophosphorus pesticides. Thus the reaction yield is low in the temperature range $T_g = 150\text{--}320^\circ\text{C}$ (<5% relative abundance). At $T_g > 340^\circ\text{C}$ thermal decomposition occurs and leads to undefined products.

The PI mass spectra of the herbicide buminafos show a protonated molecular ion of very low abundance (m/z 348) and a significantly higher fragmentation level (see Fig. 5). The tentative ion structures can be explained as follows (Fig. 6). The phosphonic diester 6 is readily cleaved at the P–C bond to give the phosphoric diester 7 and the carbenium-iminium ion 8 after proton addition. The mass spectra are dominated by the ions corresponding to the phosphoric diester 7, viz., $[\text{F} + \text{H}]^+$ (m/z 195) and $[\text{F} + \text{NH}_4]^+$ (m/z 212). The intermediate 8 undergoes direct elimination to the enamine 10, followed by gas-phase ionization (m/z 154).

The relative abundance of the $[\text{F} + \text{H}]^+$ ion with respect to the $[\text{F} + \text{NH}_4]^+$ ion depends strongly on the interface temperatures (both T_g and T_v), as can be seen from Fig. 5. However, the intensity of the quasi-molecular ion at m/z 348 is very low at each temperature, indicating

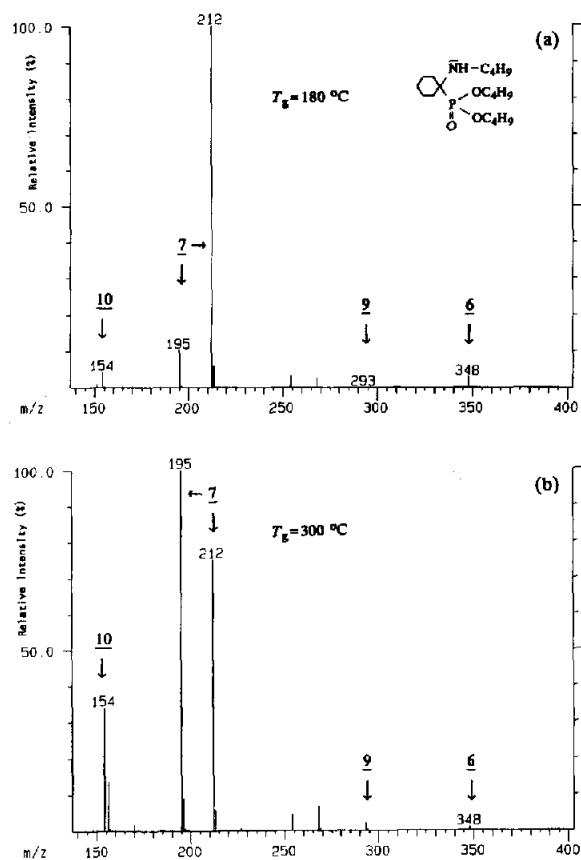


Fig. 5. TSP PI mass spectra of buminafos for different gas-phase temperatures: $T_g =$ (a) 180 and (b) 300°C. Amount injected, 600 ng. See Fig. 6 for tentative identification.

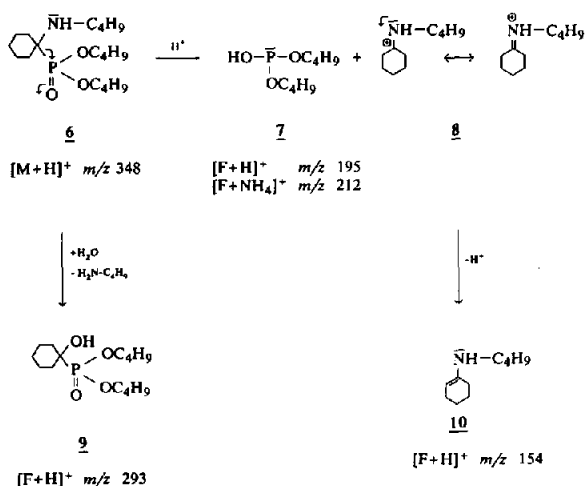


Fig. 6. Proposed fragmentation scheme for the GDR-specific herbicide buminafos and observed ions in the TSP PI mass spectra.

that dissociation occurs in the liquid phase during vaporization (in principle this dissociation could already occur during the chromatography, but the observation of only one sharp peak in the chromatogram rules this possibility out; another possibility, the decomposition of the quasi-molecular ion, is not probable in this instance because buminafos is known to dissociate readily in aqueous solution at low or high pH to give the phosphoric diester). The small signal at m/z 293 can be attributed to a hydrolysis of the N-C bond of the neutral molecule to give **9** (Fig. 6), although this reaction is not a major channel for the production of fragments even at higher temperatures.

In contrast, the PI mass spectrum of azinphos-ethyl exhibits a fragment ion (m/z 160) particularly at higher gas-phase temperatures (see Fig. 7

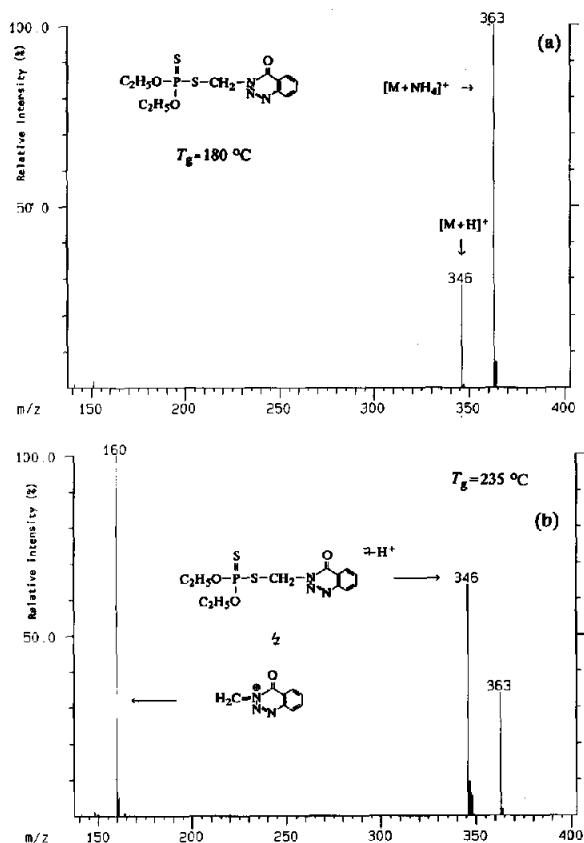


Fig. 7. TSP PI mass spectra of azinphos-ethyl for different gas-phase temperatures and proposed structure of the fragment ion. $T_g =$ (a) 190 and (b) 235°C. Amount injected, 300 ng.

for 180°C versus 235°C), which can be attributed to the decomposition of the quasi-molecular ions (m/z 346 and 363). Roach and Andrzejewski [28] have shown that azinphos analogues generally show a daughter ion of 160 u in the CAD spectra of the $[M + H]^+$ parent ions. Surprisingly, this ion is formed from the $[M + H]^+$ and/or the $[M + NH_4]^+$ ion under regular TSP conditions, whereas in the spectra of similar compounds, e.g., phosmete and phorate, no such ions are observed (Table I).

The TSP mass spectra of most of the investigated organophosphorus compounds exhibit the $[M + NH_4]^+$ and $[F + NH_4]^+$ ions as the base peak even at higher values of T_g . This is due to the proton affinity (PA) of these compounds, which is lower than that of ammonia. As an exception, the phosphorodithioates dimethoate, disulfoton and phorate show $[M + H]^+$ ions as the base peaks at each investigated temperature (see Table I for mass assignment and relative abundances). This can be attributed to the higher gas-phase basicity and PA of these compounds in comparison with phosphorothioates and phosphates, owing to the lower electronegativity of the sulphur atom instead of the oxygen atom.

Summarizing the results, one can state that many of the fragment ions in the TSP mass spectra of organophosphorus compounds are due to proton or ammonium adduct ions of thermally induced degradation products generated in the vaporizer probe or in the ion source. Lowering the gas-phase temperature leads to an increase in the quasi-molecular ion intensities for several organophosphorus pesticides as fragmentation is reduced. However, lowering T_g to $<200^\circ\text{C}$ leads to an increase in noise. Therefore, one has to find a temperature where the signal-to-noise ratio reaches an optimum. This increase in noise is probably caused by the more difficult formation of primary ions owing to a more difficult and interfered desolvation of the droplets when the spray was expanded in a “cold” ion source, i.e., for $T_g < T_v$ ($T_v \approx 200^\circ\text{C}$). Generally, we observed a decreasing noise for $T_g > T_v$ with a minimum value at $T_g \approx 235^\circ\text{C}$ and $T_s \approx 250^\circ\text{C}$ for most of the investigated pesticide compound classes. However, for azinphos-ethyl, butonate and trichlorfon one has to take the above-

mentioned fragmentations into account when performing selected-ion monitoring (SIM) experiments. Thus for these compounds we found optimum temperatures of $T_g \approx 220^\circ\text{C}$ and $T_s \approx 235^\circ\text{C}$.

Thermally induced chemical reactions during thermospray vaporization and ionization. TSP is often described as a “soft” ionization method that leads to little fragmentation. Although this may be true as far as a fragmentation of quasi-molecular ion is concerned, the examples shown above demonstrate that TSP mass spectra may contain abundant fragments where, however, dissociation is predominantly induced by chemical reactions of the neutral species which may be assisted by heat, solvent or buffer ions in the liquid phase of the vaporizer probe or in the gas phase of the ion source. In the following these fragmentations are termed “chemical dissociations”. Examples for “chemical dissociations” of neutral molecules during TSP ionization including hydrolysis, acetolysis and eliminations have also been reported by other workers [29–31]. Further examples will demonstrate that fragmentation must be considered in TSP mass spectra even at low interface temperatures.

As an example, the TSP PI mass spectra of the N-heterocyclic compound terbacil is dominated by fragment ions at m/z 161 and 178 while the quasi-molecular ion abundances at m/z 217 ($[M + H]^+$) and 234 ($[M + NH_4]^+$) are low ($<10\%$). This behaviour can be explained by the fact that the C–N bond is readily hydrolysed and/or isobutene is eliminated in the vaporizer probe or gas phase. Decreasing the vaporizer temperature T_v increases the quasi-molecular ion intensities whereas raising the gas-phase temperature probably promotes the loss of isobutene in the gas phase and hence a decrease in the quasi-molecular ion intensities is observed (see Table I and Fig. 8 for $T_g = 200^\circ\text{C}$ versus 300°C).

The dominant ion in the TSP mass spectra of the carbamate asulam (Fig. 9a) appears at m/z 190 and corresponds to an ammonium cationized fragment molecule ($[F + NH_4]^+$) with a corresponding proton adduct ion (m/z 173 = $[F + H]^+$) over the entire temperature range investigated (variation of both T_g and T_v). Asulam is probably hydrolysed during the vaporization

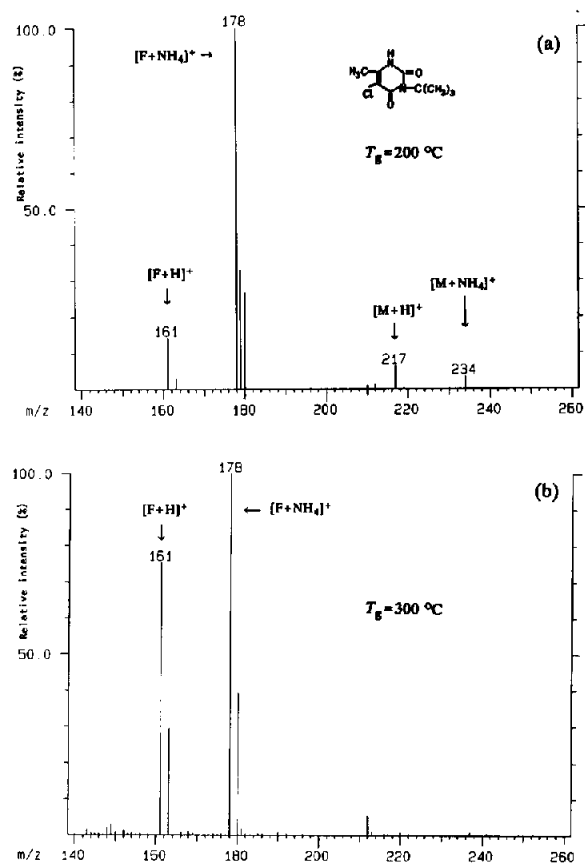


Fig. 8. TSP PI mass spectra of terbacil for $T_g =$ (a) 200 and (b) 300°C. Amount injected, 600 ng.

leading to the sulphonamide and the carbonic ester (Fig. 9a). The hydrolysis reaction was confirmed by LC-TSP-MS-MS experiments using the quasi-molecular ion $[M + NH_4]^+$ (m/z 248) as the parent ion and a low collision offset of 10 V. The daughter ions obtained are summarized in Table II (the tentative structures of the ions are presented in Fig. 9b). The ions corresponding to the degradation product are observed only in the TSP spectra and not in the CAD spectra. The ion at m/z 156 in the CAD daughter ion spectrum is probably the resonance stabilized species shown in Fig. 9b which is formed by cleavage of the S–N single bond of ionized asulam. The CAD analysis suggests that asulam, once ionized, exclusively gives the ion at m/z 156 and does not undergo a dissociation of the C–N single bond, whereas this reaction is preferred by

TABLE II

TSP POSITIVE-ION CAD DAUGHTER ION SPECTRA OBTAINED FROM THE INVESTIGATED PESTICIDES

CAD conditions: COFF, 10 V; collision cell pressure (argon), $1.3 \cdot 10^{-3}$ Torr.

Compound	Parent ion	m/z	Daughter ion spectrum: m/z (relative abundance, %)	
Alachlor	$[M + H]^+$	270	270 (40)	
			238 (100)	
	$[M + NH_4]^+$	287	270 (100)	
			238 (98)	
			162 (5)	
			238 (100)	
			224 (5)	
			220 (5)	
			208 (5)	
			162 (80)	
Asulam	$[M + NH_4]^+$	248	231 (95)	
			214 (5)	
			156 (100)	
Desmedipham	$[M + NH_4]^+$	318	182 (5)	
			137 (100)	
			94 (3)	
		$[M + NH_4]^+$	318 ^a	137 (55)
			120 (15)	
Oxamyl	$[M + NH_4]^+$	237	94 (100)	
			163 (2)	
			90 (58)	
			72 (100)	

^a COFF 30 V.

the neutral molecule probably by means of a hydrolysis in the liquid phase of the vaporizer probe.

A further example will demonstrate that raising T_g promotes "chemical dissociations". The TSP mass spectrum of the anilide alachlor **12** exhibits the quasi-molecular ions $[M + H]^+$ (m/z 270) and $[M + NH_4]^+$ (m/z 287) almost exclusively at gas-phase temperatures lower than 200°C (Fig. 10a). However, at higher values of T_g the fragmentation increases significantly (Fig. 10b and c). The TSP mass spectra are dominated by the loss of 32 and 44 u, which can be attributed to the degradation reactions presented in

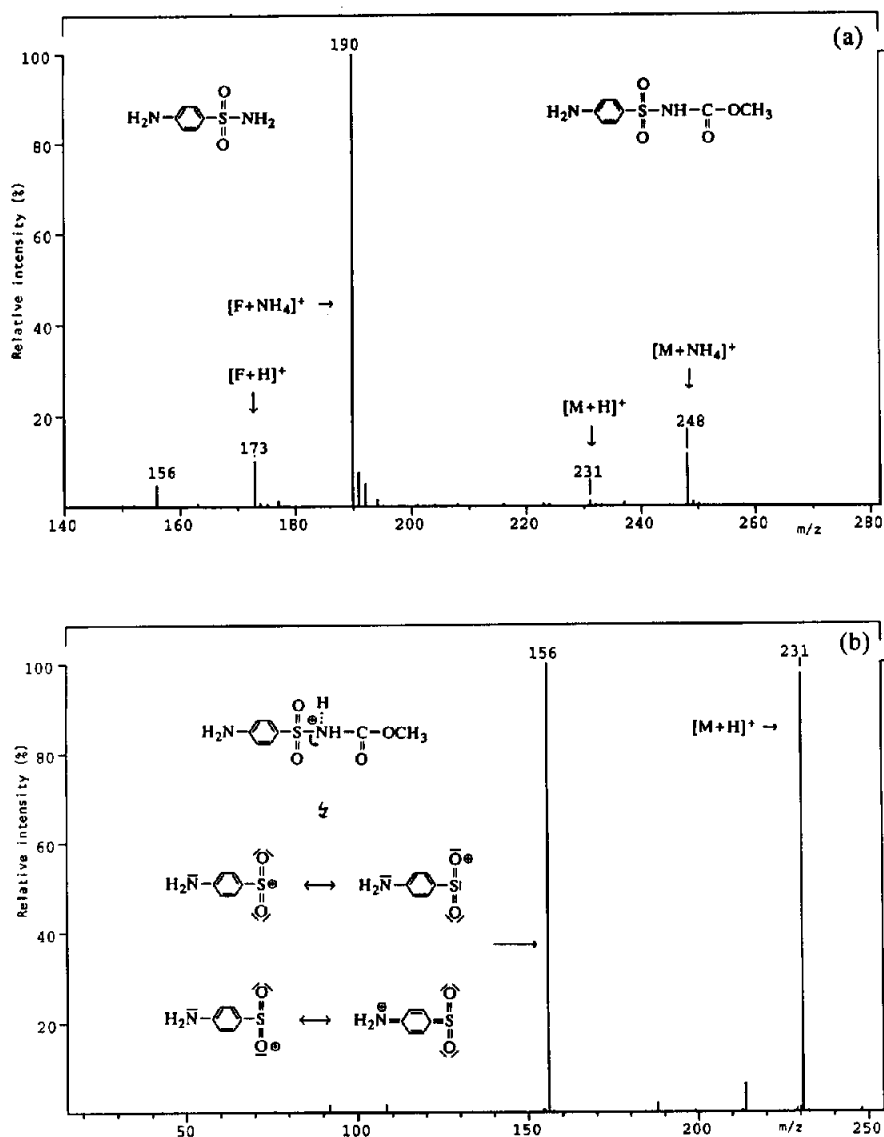


Fig. 9. CAD TSP mass spectra of asulam. (a) TSP PI spectrum and (b) daughter ion spectrum (parent ion at m/z 248). Amount injected, 100 ng.

Fig. 11. These reactions show a strong dependence on T_g as can be seen from Fig. 10a–c. Two different reaction mechanisms are probable: on the one hand a decomposition of the quasi-molecular ion $[M+H]^+$ of **12**, which gives the resonance-stabilized carbenium-imminium ion **14** at m/z 238, and on the other a simple hydrolysis reaction of the neutral tertiary amine, which leads to the secondary amine **13** with the corresponding $[F+H]^+$ and $[F+NH_4]^+$ ions in the PI

spectra, *viz.*, m/z 226 and 243. The latter was confirmed by the fact that during the low-energy CAD experiments (COFF 10 V) of the parent ions $[M+H]^+$, $[M+NH_4]^+$ and **14**, no ions are formed that can be attributed to the loss of 44 u (Fig. 12 and Table II). These results are consistent with hydrolysis of alachlor prior to ionization.

The TSP mass spectra of several N-substituted carbamates show abundant fragments even at

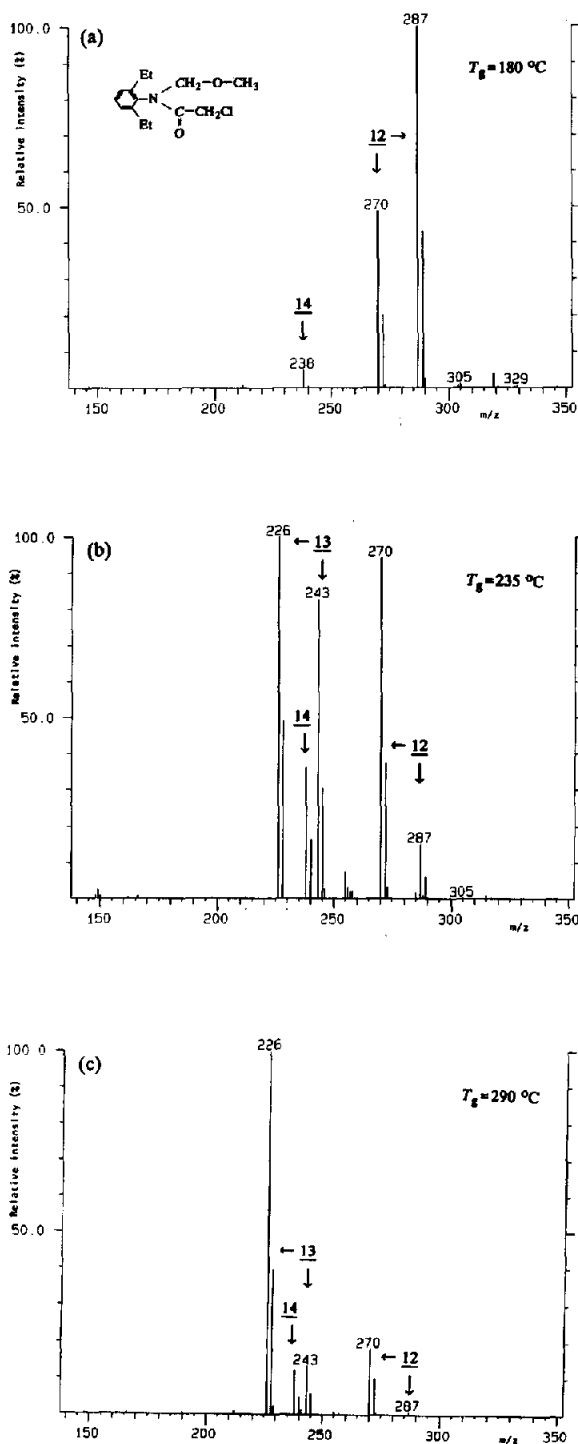


Fig. 10. TSP PI mass spectra of alachlor for different gas-phase temperatures: T_g = (a) 180; (b) 235; (c) 290°C (see Fig. 11). Amount injected, 600 ng.

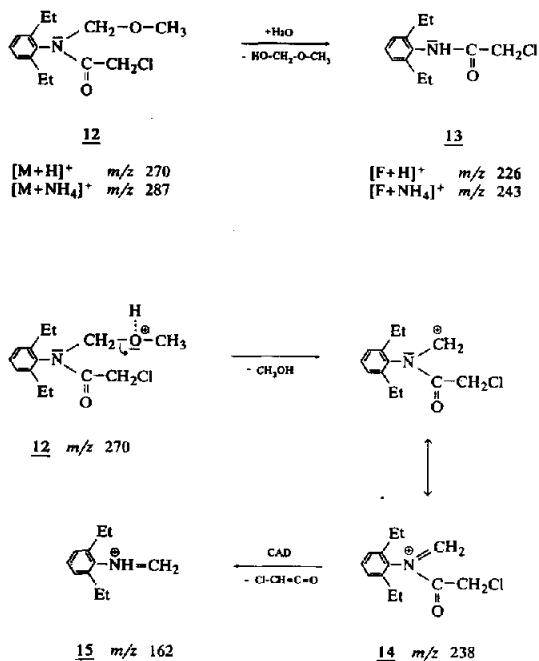


Fig. 11. Dissociation pathways for the anilide alachlor.

low vaporizer and gas-phase temperatures. These fragment ions are mainly due to the loss of the isocyanate group from the quasi-molecular ion, although fragmentation can also be explained by means of a reaction of the neutral carbamates in the liquid or gas phase. Stamp *et al.* [32] proposed a major fragmentation pathway for carbamates from CI mass spectral data which involves a proton-bound bimolecular complex (Fig. 13). This mechanism yields structurally related protonated product ions 17 and 18 which are due to the isocyanate and the alcohol formed (Table III). The weak signals at m/z 145 and 165 in the TSP PI mass spectra of carbaryl and carbofuran can probably be explained by means of this mechanism. They can be attributed to the loss of neutral methyl isocyanate from the protonated molecular ion 16. However, in the TSP PI mass spectra of desmedipham, phenmedipham and oxamyl, abundant ammonium adduct ions of the alcohol and the isocyanate are observed in addition to the protonated product ions. As an example, the TSP mass spectra of oxamyl exhibit the $[\text{M} + \text{NH}_4]^+$ ion as the base peak (m/z 237) for low values of T_g . However,

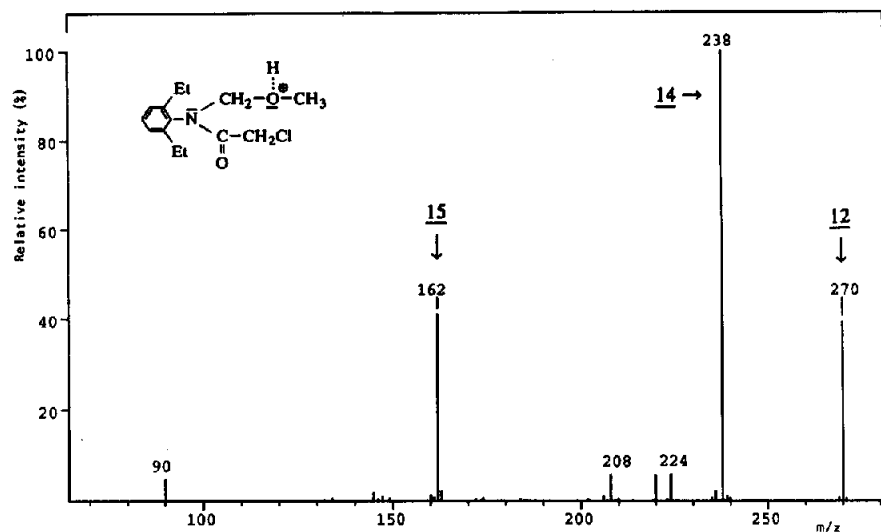
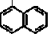
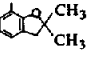


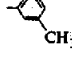


Fig. 12. CAD daughter ion spectrum of alachlor (parent ion at m/z 287).

TABLE III

DEGRADATION PRODUCTS OF N-SUBSTITUTED CARBAMATE PESTICIDES OBTAINED FROM THE TSP AND CAD SPECTRA

Carbamate	$R^1-NH-C(O)O-R^2$	Observed product ions (m/z) ^a	
		$[R^1-NCO + X]^+$	$[R^2-OH + X]^+$
Carbaryl	$R^1 = CH_3$	— ^b	
	$R^2 =$ 		145
Carbofuran	$R^1 = CH_3$	— ^b	
	$R^2 =$ 		165, 182
Desmedipham	$R^1 =$ 	120, 137	
	$R^2 = C_2H_5O-C(=O)-NH-$ 		182, 199
Phenmedipham	$R^1 =$ 	134, 151	
	$R^2 = CH_3O-C(=O)-NH-$ 		168, 185
Oxamyl	$R^1 = CH_3$	— ^b	
	$R^2 = (CH_3)_2N-CO-C(=N)-$ 		163, 180

^a X = H⁺ or NH₄⁺.^b Note: detection of ammonia and/or proton cationized methyl isocyanate was not possible under regular TSP recording conditions.

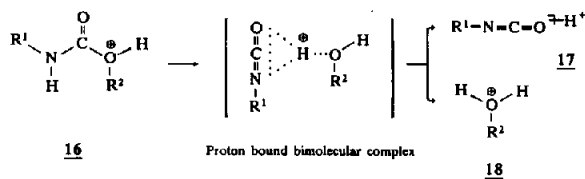


Fig. 13. Dissociation pathway for N-substituted carbamate pesticides (from Stamp *et al.* [32]).

with increasing temperature the fragment ions at m/z 163 and 180 become more abundant (Fig. 14). These ions can be attributed to the proton and ammonium adduct ion of the alcohol formed. It is probable that these ions correspond to the loss of isocyanate from the $[M + H]^+$ and $[M + NH_4]^+$ quasi-molecular ions, but the mechanism is not yet clear. Further, the spectra of the dicarbamates desmedipham and phenmedipham contain less abundant quasi-molecular ions and significantly more ammonium and proton cationized fragment ions (Table III). The intensity of the quasi-molecular ion $[M + NH_4]^+$ is low in each instance ($<5\%$ relative abundance). The base peak is due to the fragment ion at either m/z 182 or 199 for desmedipham (m/z 168 and 185 for phenmedipham), the abundance of which depends on T_g and which can be attributed to the formed alcohol. The ions at m/z 137 and 151 are probably due to the ammonium adducts of the isocyanates. These results were confirmed by performing additional CAD experiments (Table II). As an example, the CAD daughter ion spectrum of oxamyl (parent ion at m/z 237) and the structures of the ions formed are shown in Fig. 14c. The results are in agreement with those of other workers [22]. The ions at m/z 72 and 90 can be attributed to fragments formed from the protonated alcohol after the loss of methyl isocyanate. In the CAD spectra of desmedipham the ions formed compare well with those obtained from the normal TSP spectra (Table II), although no ammonium adduct ions of the alcohol fragments are observed in the CAD spectra even with the low COFF of 10 V.

The examples discussed in this and the preceding section clearly confirm the conclusion that "chemical dissociations" in the vaporizer probe or the ion source are predominantly responsible for the fragments observed in the TSP mass

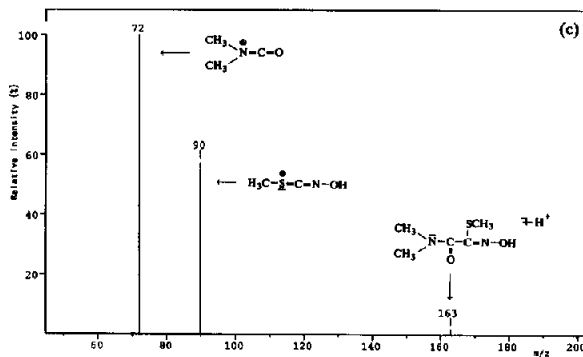
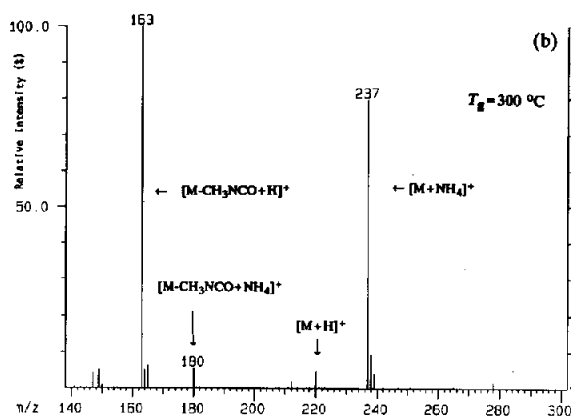
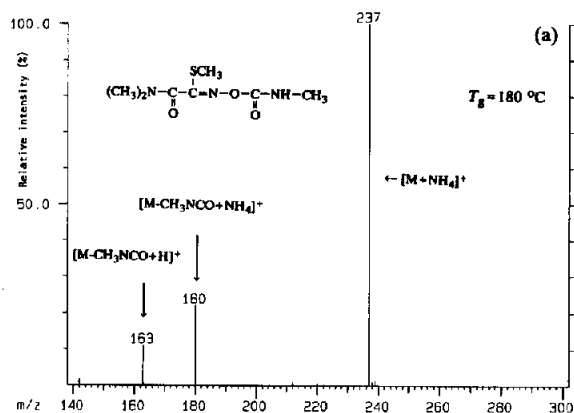
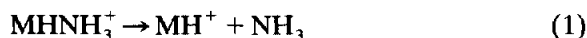


Fig. 14. TSP PI mass spectra of oxamyl for $T_g =$ (a) 200 and (b) 300°C and (c) CAD daughter ion spectrum (parent ion at m/z 237). Amount injected, 200 ng.

spectra of the investigated pesticides, particularly at lower temperatures. In many instances fragment ions formed by such “chemical dissociations” dominate the TSP mass spectra. In these instances the intensities of the quasi-molecular ions can often be increased by lowering T_g , whereas lowering T_v is not recommended in most instances because the sensitivity decreases drastically at temperatures lower than the take-off temperature (*i.e.*, at the point of complete vaporization). However, in some instances fragmentation is unavoidable (*e.g.*, asulam, desmedipham and terbacil). Hence for quantification in the SIM mode these fragment ions have to be used.

Ion abundance ratio of the quasi-molecular ions $[M + H]^+$ and $[M + NH_4]^+$. As mentioned in the previous sections, the relative intensity of the quasi-molecular ions $[M + H]^+$ and $[M + NH_4]^+$ is strongly dependent on the gas-phase temperature T_g for several carbamates, phenylureas and organophosphorus compounds (see Figs. 2, 5, 7–10, 14 and 17) where with increasing temperature $[M + H]^+$ becomes more abundant, *i.e.*, a dissociation of $[M + NH_4]^+$ leads to $[M + H]^+$:



It was observed that as T_g is raised the ion abundance ratio of the $[M + H]^+$ relative to the $[M + NH_4]^+$ ions, $r(M)$, increases exponentially whereas the sum of the ion currents of both quasi-molecular ions remains almost constant, as can be seen from Fig. 15, in which the absolute ion intensities of the different quasi-molecular ion species of chlorpropham and buminafos are plotted against T_g . For most investigated compounds the dependence of $r(M)$ on T_g can be described by the equations

$$r(M) = \frac{I[M + H]^+}{I[M + NH_4]^+} = A e^{-C/T_g} \quad (2)$$

$$\ln r(M) = \ln A - C/T_g \quad (3)$$

Thus a plot of $\ln r(M)$ against $1/T_g$ leads to a straight line in the investigated temperature range $T_g = 150\text{--}320^\circ\text{C}$. Examples of this behaviour are summarized in Fig. 16a–c for several

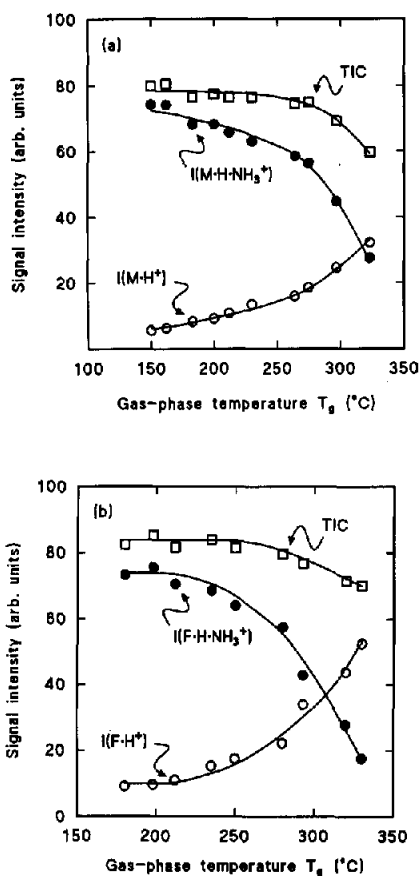
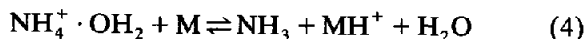


Fig. 15. Absolute quasi-molecular ion intensities and total ion current as a function of the gas-phase temperature T_g for (a) the MH^+ (m/z 214) and $(MHNH_3)^+$ (m/z 231) ions of chlorpropham (see Fig. 17) and (b) the FH^+ (m/z 195) and $(FHNH_3)^+$ (m/z 212) ions of the phosphoric diester 7 formed from buminafos (see Fig. 5).

pesticides which show combinations of both quasi-molecular ions in the TSP mass spectra.

Alexander and Kebarle [33] used the $NH_4^+ \cdot OH_2$ ion as a representative primary cluster ion for gas-phase protonation, although other cluster ions with different cluster dissociation energies, D_c , and proton affinities, PA , may be involved. Using this primary ion the processes leading to protonation and ammonium addition are described by the equations



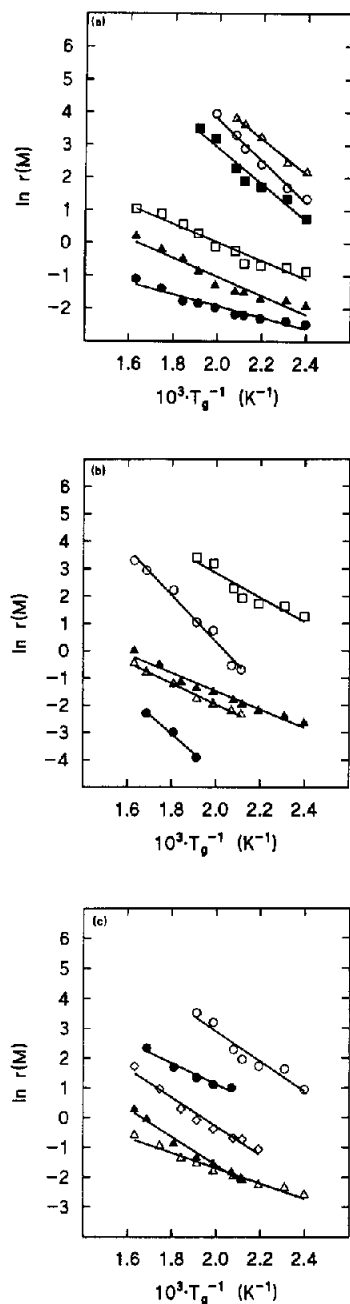
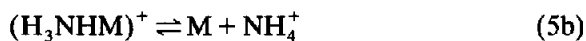


Fig. 16. $\ln I(\text{MH}^+)/I(\text{MHNH}_3^+) [= \ln r(\text{M})]$ as a function of the reciprocal of the absolute temperature of the gas phase for several pesticides. (a) ● = Carbaryl; ■ = fenuron; □ = desmedipham; ○ = methabenzthiazuron; ▲ = phenmedipham; △ = difenoxuron. (b) ● = Azinphos-ethyl; △ = trichlorphon; □ = oxamyl; ● = naled; ▲ = chlorpropham. (c) ○ = Chlorotoluron; ▲ = buminafos; ● = terbacil; ◇ = alachlor; △ = butonate.



Protonation of M according to eqn. 4 is only possible if $PA(\text{M})$ is $\geq 224 \text{ kcal mol}^{-1}$ ($\Delta H_4 = D_c + PA(\text{NH}_3) - PA(\text{M})$, where $PA(\text{NH}_3) = 204 \text{ kcal mol}^{-1}$ and $D_c \approx 20 \text{ kcal mol}^{-1}$ [33]) ($1 \text{ kcal} = 4.184 \text{ kJ}$). In this case no $[\text{M} + \text{NH}_4]^+$ signal is observed as found for N-heterocyclic pesticides, morpholines, many anilides and carbamates and some other pesticide classes. Compounds with a PA in the range $204\text{--}224 \text{ kcal mol}^{-1}$ will undergo reactions 5 and 5a. The TSP mass spectra show both $[\text{M} + \text{H}]^+$ and $[\text{M} + \text{NH}_4]^+$ ions if their PA is equal to or slightly higher than $PA(\text{NH}_3)$ as found for phenylureas and some organophosphorus compounds (e.g., the dithiophosphorus esters dimethoate, disulfoton and phorate). The equilibrium described by reaction 5a and thus the ratio $r(\text{M})$ depends sensitively on T_g , where $r(\text{M})$ can be described by eqns. 2 and 3. Compounds having PA slightly less than ammonia ($PA < 204 \text{ kcal mol}^{-1}$) can give reactions 5a and 5b. Thus, the $[\text{M} + \text{NH}_4]^+$ ion dominates the spectra, as is found for most phosphorus and phosphonic esters where eqns. 1–3 are still valid. However, if $PA(\text{M})$ is $20\text{--}30 \text{ kcal mol}^{-1}$ lower than $PA(\text{NH}_3)$, no analyte ions are formed [34].

The parameters A and C in eqns. 2 and 3 as determined from the temperature dependence of the investigated pesticides are summarized in Table IV. The correlation coefficient demonstrates that the ion intensity ratio $r(\text{M})$ can be well described by eqn. 3 for almost all compounds. However, at gas-phase temperatures $> 320^\circ\text{C}$ deviations from eqn. 3 are observed which can be attributed to undefined thermal decompositions. Even a variation of the vaporizer temperature influences $r(\text{M})$ because T_g is directly influenced by T_v . Eqn. 3 is also valid for other solvent compositions, although the values of the parameters A and C change slightly.

In general, at higher gas-phase temperatures ($T_g = 250\text{--}300^\circ\text{C}$) the TSP mass spectra of most investigated pesticides exhibit $[\text{M} + \text{H}]^+$ ions and $[\text{F} + \text{H}]^+$ ions as base peaks (with the exception of several organophosphorus pesticides), whereas at lower temperatures the $[\text{M} + \text{NH}_4]^+$ ion often dominates. These effects have to be taken

TABLE IV
EXPERIMENTAL FIT PARAMETERS A AND C (EQN. 3)

Compound	M_r [M(F)] ^a	-C	ln A	-r ^b
Alachlor	269	2.5761	3.4509	0.9838
Azinphos-ethyl	345	4.4557	11.7455	0.9945
Buminafos	195	4.7221	7.8154	0.9895
Carbaryl	201	1.7488	1.5734	0.9967
Chlorpropham	213	3.3679	5.2527	0.9425
Chlorotoluron	212	5.0495	12.9934	0.9602
Desmedipham	181	2.8015	5.6146	0.9709
Difenoxuron	286	5.3706	14.9647	0.9947
Fenuron	164	5.5814	14.0559	0.9778
Methabenzthiazuron	206	6.4229	16.6071	0.9930
Naled	380	7.0916	9.7122	0.9922
Phenmedipham	150	2.8680	4.6961	0.9662
Oxamyl	162	8.4902	17.3094	0.9909
Terbacil	160	3.5217	8.1583	0.9785
Trichlorphon	256	3.8667	5.7569	0.9944

^a Molecular mass of the molecule (M) or fragment (F).

^b Correlation coefficient.

into account when pesticides are determined in the SIM mode because the total ion current (*i.e.*, the sum of both quasi-molecular ions) is less dependent on T_g than the ion current of the individual quasi-molecular ions (see Fig. 15a and b).

Additional adduct ions. According to Maeder [35], TSP PI quasi-molecular ions $[M_{qm}]^+$ have the general formula

$$[M_{qm}]^+ = [M + A + xB - yC]^+ \quad (6)$$

where M is the nominal mass of the analyte molecule, A is the attached ion (*e.g.*, H^+ , NH_4^+), B is the attached solvent molecule (H_2O , $MeOH$) and/or additive molecule (NH_4OAc , $HCOONH_4$), C is the eliminated molecule (H_2O , $MeOH$) and x and y are integers beginning with zero.

We investigated the ion abundance of several pesticides in the temperature range $T_g = 150$ – $320^\circ C$. As an example, the TSP PI mass spectra of four phenylurea and carbamate pesticides are shown in Fig. 17a–d for $T_g = 150^\circ C$. All compounds give adduct ions which can in part be explained by applying eqn. 6. The base peak was the $[M + H]^+$ ion and the second most abundant ion was the $[M + NH_4]^+$ ion for the phenylureas.

This is also the case for some other investigated phenylureas, the spectra of which are not shown here. This is in contrast to reports by other workers [18,36], who found that $[M + NH_4]^+$ is always the base peak for phenylurea herbicides. This difference is probably due to the different designs of the ion sources, whereas the use of different ionization media (filament-off, filament, discharge) has only a slight influence on the abundance ratios of the quasi-molecular ions. Chlorpropham exhibits $[M + NH_4]^+$ as the base peak. At lower gas-phase temperatures additional adduct ions besides the “normal” quasi-molecular ions such as $[M + MeOH + H]^+$ and $[M + NH_4OAc - 2H_2O + H]^+$ appear in the spectra with relative abundances of *ca.* 2–15% (see Table I for mass assignment). These ions follow eqn. 6. In addition, we found an $[M + 46]^+$ ion which is not described by eqn. 6 and the origin of which at present is not clear. In the spectra of the anilide alachlor different adduct ions can be observed which, however, are still in agreement with eqn. 6 (Table I and Fig. 10).

For all phenylureas the $[M + H]^+$ ion remains the base peak when T_g is raised while the $[M + NH_4]^+$ is still present. However, the other adduct ions completely disappear at $T_g > 200^\circ C$,

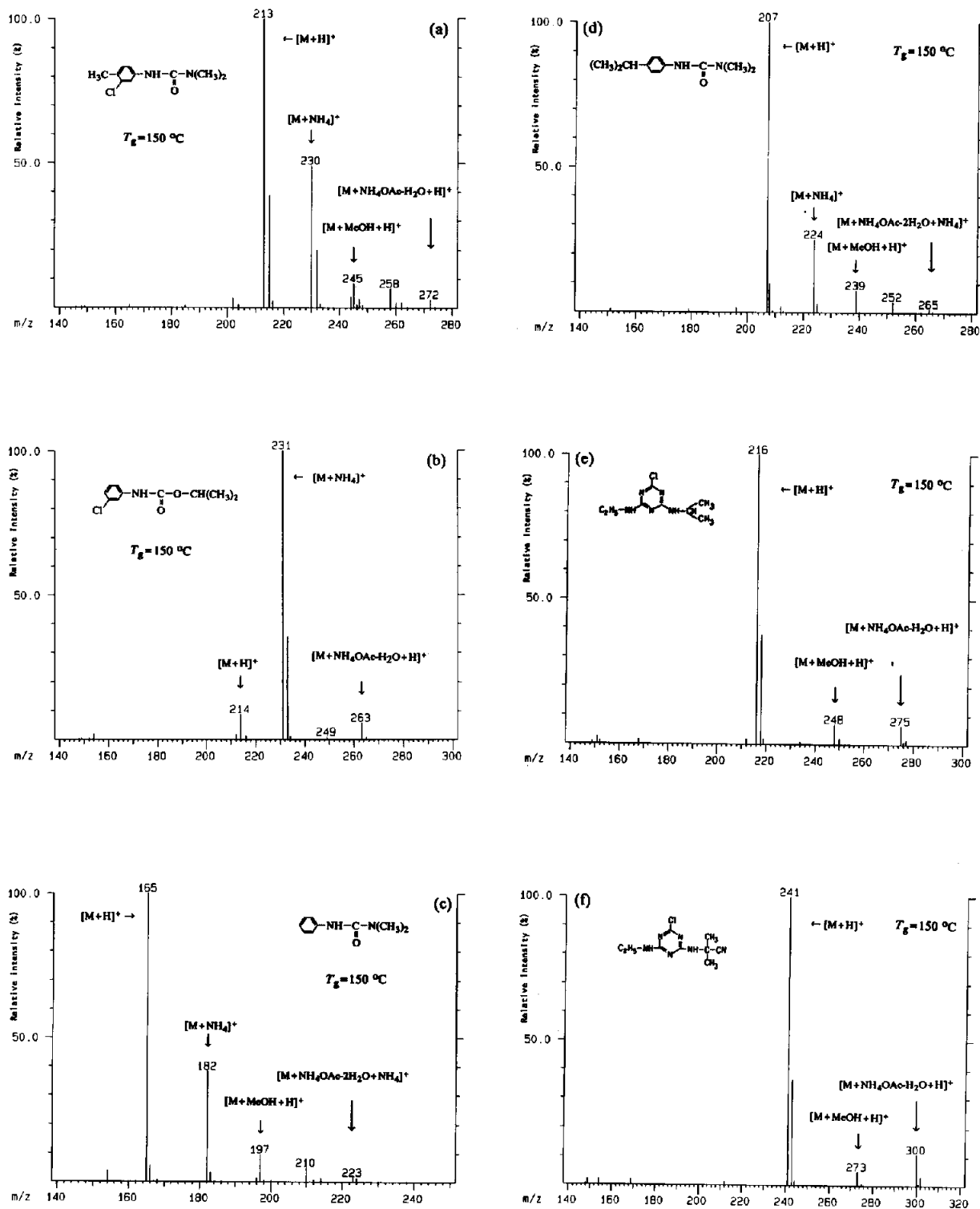


Fig. 17. TSP PI mass spectra of (a) chlorotoluron, (b) chlorpropham, (c) fenuron, (d) isotoproturon, (e) atrazine and (f) cyanazine for $T_g = 150\text{ }^\circ\text{C}$ (600 ng each).

indicating that these adduct ions undergo thermal decomposition.

Adduct ion formation and its temperature dependence were also studied for several triazine herbicides using ammonium acetate as the volatile buffer salt. The adduct ion formation can be rationalized as described above. The TSP spectra of atrazine and cyanazine are shown as examples in Fig. 17e and f for $T_g = 150^\circ\text{C}$. The $[\text{M} + \text{H}]^+$ ion is always the base peak and no $[\text{M} + \text{NH}_4]^+$ signal is obtained, as triazine compounds have proton affinity values that are higher than that of ammonia. At lower temperatures we observed two additional adduct ions in the spectra that can be attributed to the $[\text{M} + \text{MeOH} + \text{H}]^+$ and $[\text{M} + \text{NH}_4\text{OAc} - \text{H}_2\text{O} + \text{H}]^+$ ions (see Table I) with relative abundances of ca. 10–15%. At $T_g > 200^\circ\text{C}$ these ions disappear. In contrast, Barceló *et al.* [23,36,37] observed the $[\text{M} + \text{NH}_4\text{OAc} - \text{H}_2\text{O} + \text{H}]^+$ ion as the base peak for

low gas-phase temperatures (200°C) and the $[\text{M} + \text{H}]^+$ ion at higher temperatures (270°C). As mentioned above, this difference is probably due to the different designs of the TSP sources, some of which favour high clustering with the solvent [27,36].

Under typical operating conditions ($T_s = 220\text{--}300^\circ\text{C}$ and $T_g \approx 210\text{--}290^\circ\text{C}$; see Experimental) no additional adduct ions were observed. Adduct ion formation can be used to gain additional structural information, as shown by Barceló *et al.* [23].

Dependence of the ion abundance in thermospray mass spectra on the buffer concentration. Application to quaternary ammonium herbicides

The direct flow-injection TSP mass spectra of the diquaternary ammonium herbicides diquat and paraquat using pure water and 50 mM am-

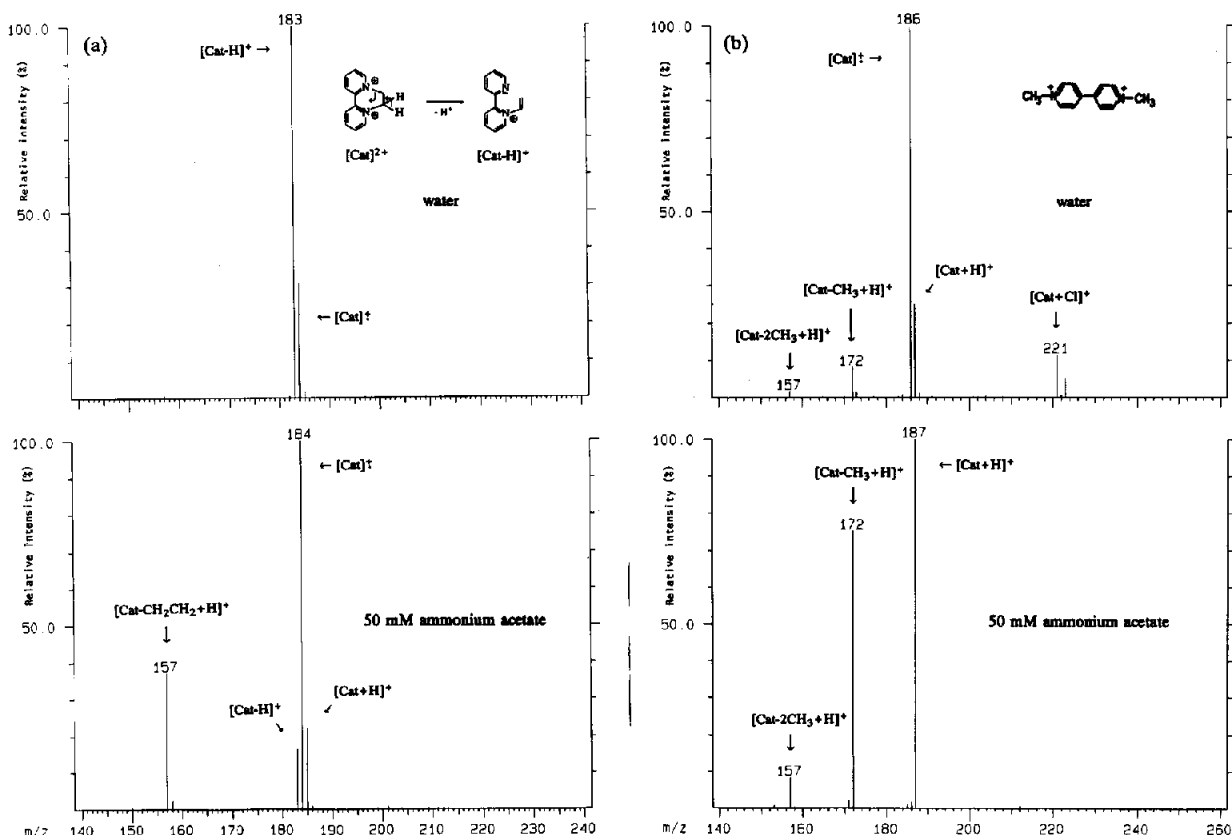


Fig. 18. Direct flow-injection TSP mass spectra of 300 ng of (a) diquat and (b) paraquat. Mobile phase: (top) water and (bottom) 50 mM ammonium acetate.

monium acetate as the mobile phase are shown in Fig. 18.

The signal at m/z 183 dominates the TSP spectra of diquat in pure water (without salt). The peak can be attributed to the unusual deprotonated dication $[\text{Cat} - \text{H}]^+$ which is probably formed by "fragmentation" of the intact dication (Fig. 18). No other ions except the intact dication (m/z 92) could be observed (Table I). This leads to the conclusion that only thermal dissociations are possible without the buffer salt.

With ammonium acetate in the mobile phase, the TSP mass spectra exhibit more ions which are due to additional chemical reactions in the gas phase induced by buffer ions. The major difference between the spectra with aqueous ammonium acetate and pure water as solvent is on the one hand the increased production of ions by reduction of the dication (formation of $[\text{Cat}]^+$) and on the other the enhanced formation of fragment ions formed by cleaving off the C_2H_4 chain (doubly positively charged!) from the dication followed by protonation of the formed neutral amine rather than loss of H^+ as shown in Fig. 18. This results in enhanced relative abundances of $[\text{Cat}]^+$, $[\text{Cat} + \text{H}]^+$ and $[\text{Cat} - \text{C}_2\text{H}_4 + \text{H}]^+$ versus $[\text{Cat} - \text{H}]^+$ and $[\text{Cat}]^{2+}$ (Fig. 18a). This behaviour can be explained by the fact that bipyridinium compounds are easily reduced to the free radicals by reducing agents [38].

In contrast to other investigations [39,40], we found an increase in the intensity of the intact dication at m/z 92 as the salt concentration c_s is raised. However, this increase is not as strong as for the monovalent reaction products.

Under TSP conditions paraquat behaves similarly to diquat, although the $[\text{Cat} - \text{H}]^+$ ion is absent (Fig. 18b). Paraquat exhibits a loss of 15 and 30 u from the intact dication owing to the loss of one or two methyl groups, simultaneously taking away one positive charge (of course, in the event of the cleavage of both methyl groups, the formed neutral molecule is protonated to give $[\text{Cat} - 2\text{CH}_3 + \text{H}]^+$). However, the signal at m/z 172 leads to the conclusion that the reduced dication is also fragmented ($[\text{Cat} - \text{CH}_3 + \text{H}]^+$). The peak at m/z 221 can be attributed to the addition of the anion (Cl^-) to the dication with the corresponding ^{37}Cl isotopic peak (m/z 223).

The dication (m/z 93) appears in the spectra only in solutions without salt addition, but the intensity is low (<5% relative abundance). The base peak can be attributed to the $[\text{Cat} + \text{H}]^+$ ion (m/z 187), while the $[\text{Cat}]^+$ ion (m/z 186) dominates in pure water.

Divalent quaternary ammonium salts can be separated on highly deactivated reversed-phase materials using methanol–water or acetonitrile–water gradient mixtures as the mobile phase. For this reason, it was of interest to investigate the behaviour of these compounds in such mixed solvents, particularly the dependence of the abundances and the intensities of the different ion species on c_s .

Results for the repetitive injection of 300 ng of paraquat using methanol–water (50:50, v/v) at

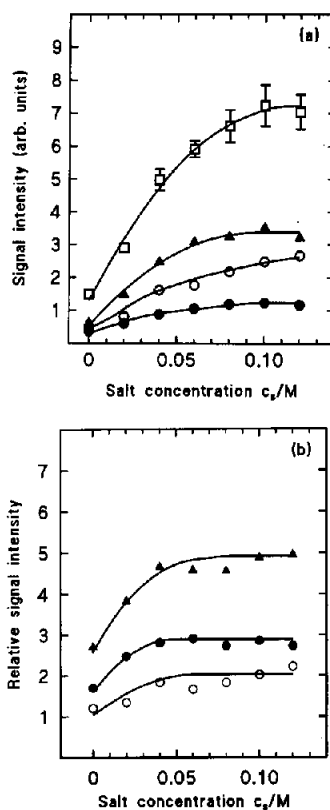


Fig. 19. (a) Absolute and (b) relative ion intensities as a function of the concentration of ammonium acetate in methanol–water (50:50, v/v) for injections of 300 ng of paraquat. (a) \square = TIC; \blacktriangle = $I([\text{M} - \text{R} + \text{H}]^+)$; \circ = $I([\text{M} - 2\text{R} + \text{H}]^+)$; \bullet = $I([\text{M}]^+ + [\text{M} + \text{H}]^+)$. (b) \blacktriangle = $I(\text{fragment ions})/I(\text{M})$; \bullet = $I([\text{M} - \text{R} + \text{H}]^+)/I(\text{M})$; \circ = $I([\text{M} - 2\text{R} + \text{H}]^+)/I(\text{M})$.

different salt concentrations are summarized in Fig. 19a and b. In Fig. 19b the ratio of the fragment ion intensity relative to the sum of the molecular ion intensity is plotted against the salt concentration. One observes that fragmentation is enhanced as c_s is raised. This phenomenon can probably be explained by considering the possibility of solid particle formation in the ion source at higher c_s and the subsequent thermal decomposition of these solid particles, thus releasing the analyte ions [40,41]. The thermal stress of the analyte molecule is apparently much higher in the solid particles and thus thermal fragmentation is enhanced. In comparison with the aqueous solution (Fig. 18), fragmentation is much higher in the case of the mixed solvent whereas the intact dication (m/z 93) is absent even without added salt. This observation leads to the conclusion that the dication is mainly degraded to the monovalent fragment ions or reduced to the monovalent cation. However, the intensity of the monovalent cation is nevertheless strongly enhanced as c_s is increased (Fig. 19a).

The use of the filament or the discharge electrode leads to unsatisfactory results in both solvents (methanol–water and pure water) because the increase in the signal intensity of all ions cannot compensate for the strong increase in the noise.

In conclusion, we do not recommend the determination of quaternary ammonium herbicides without the use of a buffer salt. The decrease in sensitivity due to fragmentations on raising the salt concentration is readily compensated for by a much higher gain in sensitivity for each ion. The curves obtained (Fig. 19a) are very similar to those reported for neutral analytes, *i.e.*, the optimum concentration of ammonium acetate is in the range 50–100 mM. When chromatographic conditions restrict high concentrations of salt, *e.g.*, for ion-exchange separations [17], one has to add the salt postcolumn.

CONCLUSIONS

The principal conclusions derived from these investigations for the determination of pesticides by means of LC–TSP–MS are the following. Organophosphorus pesticides are thermally

labile. The compounds show gas-phase thermal degradation reactions that are strongly dependent on the gas-phase temperature. These reactions are mainly due to “chemical dissociations” of the neutral precursors, followed by gas-phase protonation or ammonium addition. However, decreasing the gas-phase temperature and the ion source temperature to optimum values leads to an increase in the quasi-molecular ion abundances. Under these conditions, the compounds investigated are stable under TSP conditions, *i.e.*, the fragmentation is minimized.

The examples presented demonstrate that for some pesticide compound classes fragmentation reactions occur during TSP vaporization and ionization. However, thermal decompositions are less important in TSP mass spectra. Most bond cleavages can be explained by hydrolysis reactions and/or rearrangements and eliminations of the neutral molecules, and only in some instances of the quasi-molecular ions, induced by buffer or solvent ions which depend strongly on the gas-phase temperature, indicating the domination of gas-phase processes. In some instances these fragmentation reactions are unavoidable. However, if the reactions involved have high yields and the fragments formed reflect the structure of the original pesticide, this is not necessarily a disadvantage, especially for quantification purposes. Further, LC–TSP–MS can be used as an ideal confirmatory method in some instances.

For most of the investigated compounds a linear relationship is observed when the logarithm of the ion abundance ratio for the $[M + H]^+$ ion relative to the $[M + NH_4]^+$ ion is plotted against the reciprocal of the absolute temperature of the gas phase in the range $T_g = 150–320^\circ\text{C}$. As several pesticide compound classes show both $[M + H]^+$ and $[M + NH_4]^+$ ions, this temperature dependence can be used to generate TSP spectra with mainly one quasi-molecular ion, thus concentrating the main ion current into one instead of two ions. This may be of value in trace analyses for pesticides if the mass spectrometer is operated in the SIM mode, because the total ion current (*i.e.*, the sum of both quasi-molecular ions) is less dependent on T_g than the ion current of the individual quasi-

molecular ions.

It was found that additional adduct ions beside the quasi-molecular ions may be observed in TSP PI mass spectra of several pesticides (e.g., carbamates, organophosphorus pesticides, phenylureas and triazines). These additional ions are expected to be useful for an unambiguous identification of pesticides in real environmental samples. However, the intensity of these ions is low in each instance and the formation is limited to low gas-phase and ion source temperatures.

The results reported for the divalent quaternary ammonium herbicides demonstrate that the addition of a volatile buffer salt to the mobile phase is necessary although the compounds are already completely dissociated in the aqueous solvent. The observed relationships for the ion intensity versus salt concentration are similar to those reported for neutral molecules. Although fragmentation is enhanced as the salt concentration is raised, this disadvantage can readily be compensated for by the strong increase in sensitivity.

ACKNOWLEDGEMENTS

We thank Dr. J. Schmidt (Solvay Deutschland, Hannover, Germany) for facilitating the CAD experiments. We acknowledge financial support from the Bundesministerium für Forschung und Technologie.

REFERENCES

- 1 T.R. Covey, E.D. Lee, A.P. Bruins and J.D. Henion, *Anal. Chem.*, 58 (1986) 1451A.
- 2 K. Levens, *Org. Mass Spectrom.*, 23 (1988) 406.
- 3 L.H. Wright, *J. Chromatogr. Sci.*, 20 (1982) 1.
- 4 T. Cairns, E.G. Siegmund and G.M. Dose, *Biomed. Mass Spectrom.*, 10 (1983) 24.
- 5 R.D. Voyksner and J.T. Bursey, *Anal. Chem.*, 56 (1984) 1582.
- 6 T.R. Covey and J.D. Henion, *Anal. Chem.*, 55 (1983) 2275.
- 7 M. Barber, R.S. Bordoli, G.J. Elliot, R.D. Sledgewick and A.N. Tyler, *Anal. Chem.*, 54 (1982) 645A.
- 8 C.R. Blakely and M.L. Vestal, *Anal. Chem.*, 55 (1983) 750.
- 9 M.L. Vestal, *Anal. Chem.*, 56 (1984) 2590.
- 10 P. Arpino, *Mass Spectrom. Rev.*, 9 (1990) 631.
- 11 T.D. Behymer, T.A. Bellar and W.L. Budde, *Anal. Chem.*, 62 (1990) 1686.
- 12 S. Pleasance, J.F. Anacleto, M.R. Baily and D.H. North, *J. Am. Soc. Mass Spectrom.*, 3 (1992) 378.
- 13 T.A. Bellar and W.L. Budde, *Anal. Chem.*, 60 (1988) 2076.
- 14 E.R.J. Wils and A.G. Hulst, *Fresenius' J. Anal. Chem.*, 342 (1992) 749.
- 15 D. Barceló, *Biomed. Environ. Mass Spectrom.*, 17 (1988) 2076.
- 16 A. Farran, J. De Pablo and D. Barceló, *J. Chromatogr.*, 455 (1988) 163.
- 17 C.H. Vestal, *Vestec Thermospray Newsl.*, 3 (1987) 2.
- 18 D. Barceló, *Org. Mass Spectrom.*, 24 (1989) 219.
- 19 R.D. Voyksner, in J.D. Rosen (Editor), *Applications of New Mass Spectrometry Techniques in Pesticide Chemistry*, Wiley, New York, 1987, p. 146.
- 20 T.L. Jones, L.D. Betowsky and J. Yinon, in M.A. Brown (Editor), *Liquid Chromatography/Mass Spectrometry. Applications in Agricultural, Pharmaceutical, and Environmental Chemistry (ACS Symposium Series, No. 420)*, American Chemical Society, Washington, DC, 1990, p. 62.
- 21 R.D. Voyksner, in J.D. Rosen (Editor), *Applications of New Mass Spectrometry Techniques in Pesticide Chemistry*, Wiley, New York, 1987, p. 247.
- 22 K.S. Chiu, A. Van Langenhove and C. Tanaka, *Biomed. Environ. Mass Spectrom.*, 18 (1989) 200.
- 23 D. Barceló, G. Durand, R.J. Vreeken, G.J. De Jong, H. Lingeman and U.A.Th. Brinkman, *J. Chromatogr.*, 553 (1991) 311.
- 24 D.J. Liberato and P. Kebarle, *Anal. Chem.*, 58 (1986) 6.
- 25 R.D. Voyksner, J.T. Bursey and E.D. Pellizari, *Anal. Chem.*, 56 (1984) 1507.
- 26 T.M. Chen, J.E. Coutant, A.D. Sill and R.R. Fike, *J. Chromatogr.*, 396 (1987) 382.
- 27 D. Barceló and J. Albaiges, *J. Chromatogr.*, 474 (1989) 163.
- 28 J.A.G. Roach and D. Andrzejewski, in J.D. Rosen (Editor), *Application of New Mass Spectrometry Techniques in Pesticide Chemistry*, Wiley, New York, 1987, p. 187.
- 29 M.M. Siegel, R.K. Isensee and D.J. Beck, *Anal. Chem.*, 59 (1987) 989.
- 30 M.F. Bean, S.L. Pallante-Morell and C. Fenselau, *Biomed. Environ. Mass Spectrom.*, 18 (1989) 219.
- 31 W.M. Lagna and P.S. Callery, *Biomed. Mass Spectrom.*, 12 (1985) 699.
- 32 J.J. Stamp, E.G. Siegmund, T. Cairns and K.K. Chan, *Anal. Chem.*, 58 (1986) 873.
- 33 A.J. Alexander and P. Kebarle, *Anal. Chem.*, 58 (1986) 471.
- 34 A. Harrison, *Chemical Ionization Mass Spectrometry*, CRC Press, Boca Raton, FL, 1983, p. 33.
- 35 H. Maeder, *Rapid Commun. Mass Spectrom.*, 4 (1990) 52.
- 36 D. Barceló, *Chromatographia*, 25 (1988) 295.
- 37 D. Barceló, in M.A. Brown (Editor), *Liquid Chromatography/Mass Spectrometry. Applications in Agricultural, Pharmaceutical, and Environmental Chemistry (ACS*

- Symposium Series*, No. 420), American Chemical Society, Washington, DC, 1990, p. 48.
- 38 H.P. Thier and H. Zeumer (Editors), *Manual of Pesticide Residue Analysis*, Vol. 1, Deutsche Forschungsgemeinschaft, Pesticides Comm., VCH, Weinheim, 1987, p. 177.
- 39 T.R. Covey, A.P. Bruins and J.D. Henion, *Org. Mass Spectrom.*, 20 (1988) 178.
- 40 G. Schmelzeisen-Redeker, F.W. Röllgen, H. Wirtz and F. Voegtle, *Org. Mass Spectrom.*, 20 (1985) 752.
- 41 G. Schmelzeisen-Redeker, M.A. McDowall, U. Giessmann, K. Levsen and F.W. Röllgen, *J. Chromatogr.*, 323 (1985) 127.